CERN – EUROPEAN ORGANIZATION FOR NUCLEAR RESEARCH

CLIC – Note – 1050

RF DESIGN OF THE TW BUNCHER FOR THE CLIC DRIVE BEAM INJECTOR

Progress report according to the collaboration agreement N° KE2285/BE/CLIC

Hamed Shaker, School of particles and accelerators, IPM, Tehran - Iran

Abstract

The CLIC is based on the two beams concept that one beam (drive beam) produces the required RF power to accelerate another beam (main beam). The drive beam is produced and accelerated up to 50MeV inside the CLIC drive beam injector. The drive beam injector main components are a thermionic electron gun, three sub harmonic bunchers, a pre-buncher, a TW buncher,13 accelerating structures and one magnetic chicane. This document is the first report of the RF structure design of the TW buncher. This design is based on the beam dynamic design done by Shahin Sanaye Hajari due to requirements mentioned in CLIC CDR. A disk-loaded tapered structure is chosen for the TW buncher. The axial electric field increases strongly based on the beam dynamic requirements. This report includes the design of the power couplers. The fundamental mode beam loading and higher order modes effect were preliminary studied.

Geneva, Switzerland
09/03/2015

RF Design of the TW buncher for the CLIC drive beam injector

Progress report according to the collaboration agreement N0. KE2285/BE/CLIC

Hamed Shaker

School of particles and accelerators, IPM

Abstract

The CLIC is based on the two beams concept that one beam (drive beam) produces the required RF power to accelerate another beam (main beam). The drive beam is produced and accelerated up to 50MeV inside the CLIC drive beam injector. The drive beam injector main components are a thermionic electron gun, three sub harmonic bunchers, a pre-buncher, a TW buncher, 13 accelerating structures and one magnetic chicane. This document is the first report of the RF structure design of the TW buncher. This design is based on the beam dynamic design done by Shahin Sanaye Hajari [1] due to requirements was mentioned in CLIC CDR [2]. A disk-loaded tapered structure is chosen for the TW buncher that lets the axial electric field increases based on the beam dynamic requirement. This report also consists of the power couplers design. The fundamental mode beam loading and higher order modes effect were preliminary studied due to cells detuning for HOMs.

Introduction

The current CLIC project preparation phase foresees to study in detail the drive beam injector front end. A complete beam dynamics design as well as RF designs of the Sub Harmonic Bunchers and accelerating structres are performed. In addition prototypes of critical hardware are being built and tested. The drive beam front-end is the first part of the CLIC drive beam injector with the beam energy up to 12 MeV. Figure 1 shows its layout. The Electron gun, sub harmonic bunchers, pre-buncher and accelerating structures are designed and the first SHB is under construction. This text is the first report about the TW buncher design which was missing until now. The design of this buncher is subject of the collaboration agreement No KE2285/BE/CLIC.

A buncher, bunches and accelerates bunches simultaneously. In most design cases, when beam loss is not so critical, the bunching mechanism is less paid attention and bunches travel near the crest but in our case we need a good bunching to reduce beam loss and satellite population.

A disk-loaded waveguide structure is chosen for the TW buncher. It consists of several cells and each cell is described by four geometrical parameters: 1-Length 2-Inner radius 3- Disk aperture radius 4-Disk thickness (That is chosen equal to 10mm for all cells). By knowing the working frequency (999.5MHz) and the phase advance between cells ($2\pi/3$), these geometrical parameters could be calculated if we know the phase velocity and the magnitude of axial electric field in each cell. Finding these parameters and also the number of cells is based on the beam dynamic study that was done by Shahin[1]. After this step we can continue for the RF structure design.

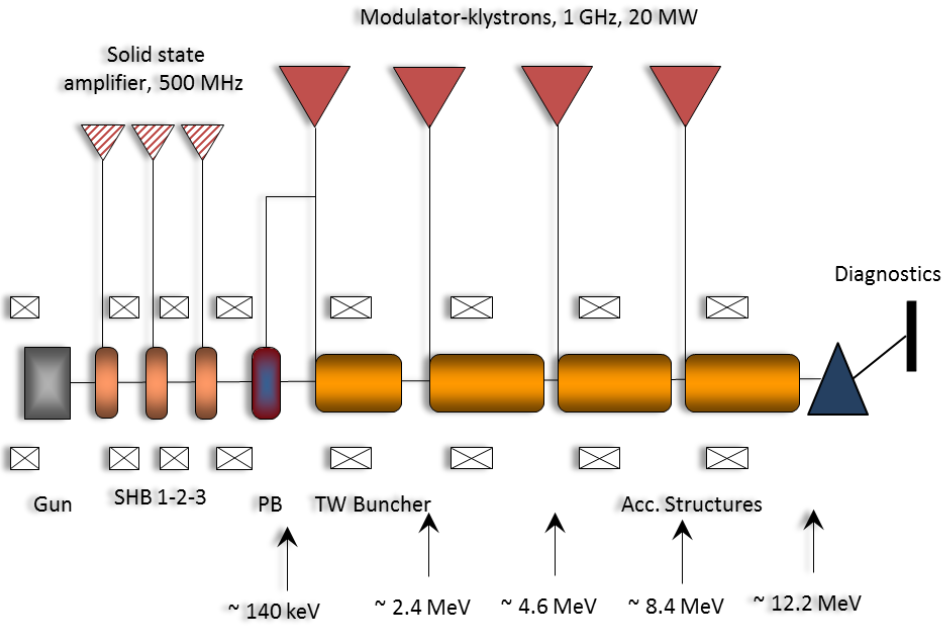

Figure 1: The drive beam front-end layout

The design based on the beam dynamics study done by Sh. Sanaye Hajari[1]

A buncher behaves like a damped oscillator. This damping is performed by smoothly increasing of axial electric field along the buncher. To have a good bunching the particles inside the bunch should have a few oscillations around the middle of the bunch then bunches should enter the structure close to zero crossing. Also to have acceleration, the phase should increase smoothly toward crest along the buncher. To increase the bunching phase acceptance the electric field at the beginning should be comparatively low to avoid kicking particles out. The electron beam energy at the entrance of the TW buncher is about 140KeV with the velocity equals to about 0.62c. The phase velocity of each cell should be equal or close to the average beam velocity in each cell.

To find the optimum values for the phase velocity and the field magnitude, we can track the particles inside the TW buncher by ignoring the space charge effect in this step and we will consider it later when we want to simulate the beam tracking by the PARMELA code. The equation below shows the dynamics of particles inside the TW buncher:

$$\begin{cases} \dfrac{d\gamma}{dz} = -\dfrac{e}{mc^2} E_z \sin\theta \\ \dfrac{d\theta}{dz} = \dfrac{\omega}{c}\left(\dfrac{1}{\beta_p} - \dfrac{1}{\beta}\right) \\ \gamma = (1-\beta^2)^{-\frac{1}{2}} \end{cases}$$

E_z,θ,β_pc,βc are the axial electric field for the main harmonic of fundamental mode, particle relative phase to the RF wave, phase velocity and particle velocity, respectively. Now if we suppose a linear phase change inside the structure and a quadratic function for the axial electric fields as mentioned

below we can find the optimum parameters that reduce the bunch length and satellite population with the maximum phase acceptance.

$$\begin{cases} E_z(z) = E_0 + E_1 z + E_2 z^2 \\ \theta_s(z) = \theta_1 z \\ \dfrac{d}{dz}\dfrac{1}{\sqrt{1-\beta_p^2}} = -\dfrac{e}{mc^2} E_z(z)\sin\theta_s(z) \end{cases}$$

Figure 2 shows the particle tracking result for the optimum case and figure 3 shows the optimum parameters. There is a constraint on the maximum electric field at the end of TW buncher that comes from the amount of the input RF power (20 MW) and the minimum group velocity (>0.01c).

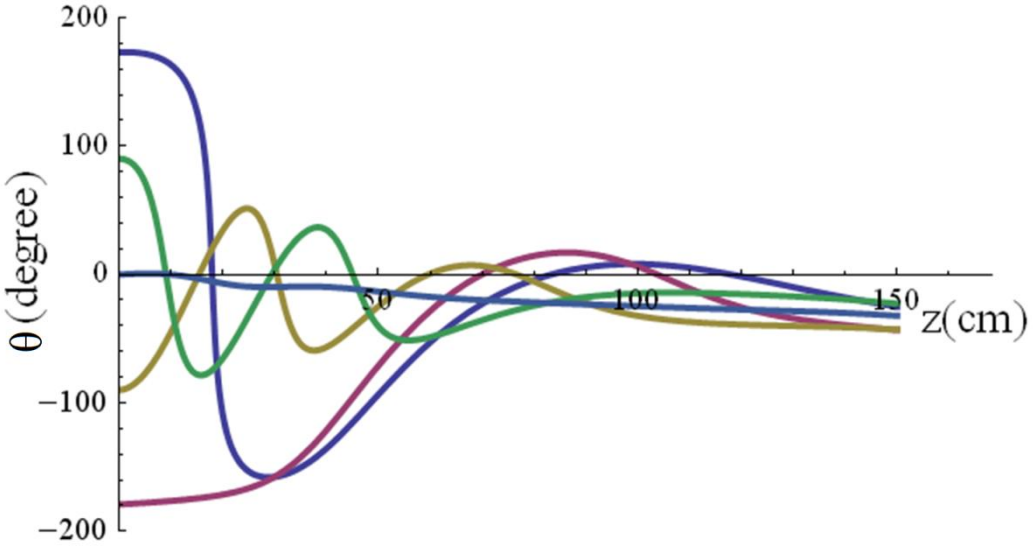

Figure 2: Particle tracking result

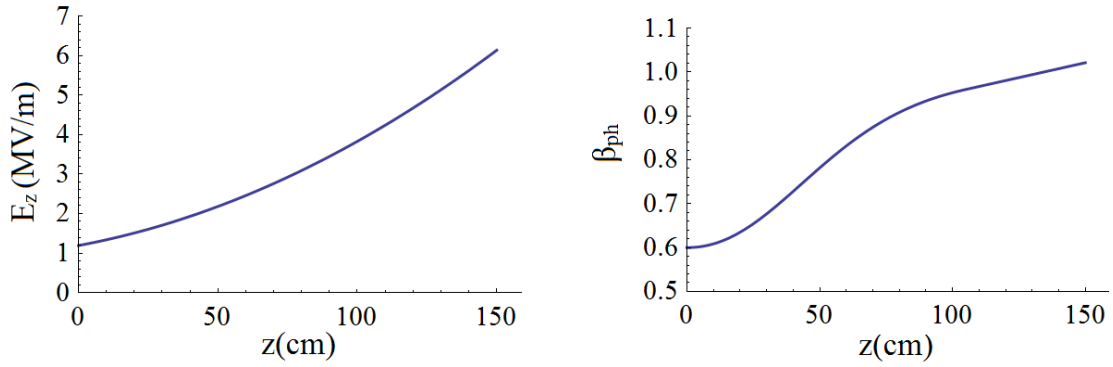

Figure 3: Optimum phase velocity and the axial electric field inside the structure

By these parameters, the beam dynamics simulation could be done by the PARMELA code with considering the space charge effect. Figures 4 and 5 show the final phase space diagrams and the table 1 shows the beam properties at the end of TW buncher. In the figure 4, the satellites are also shown.

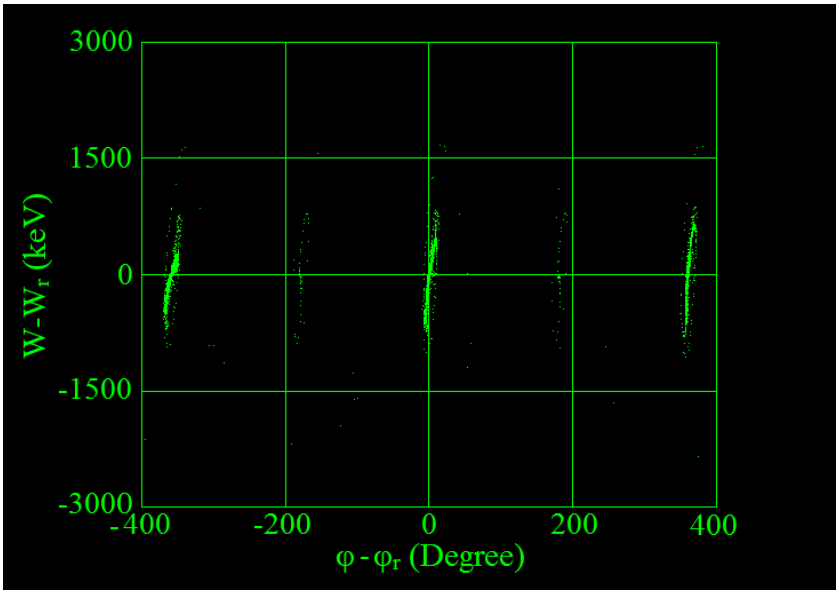

Figure 4: Phase space diagram of several bunches with satellites.

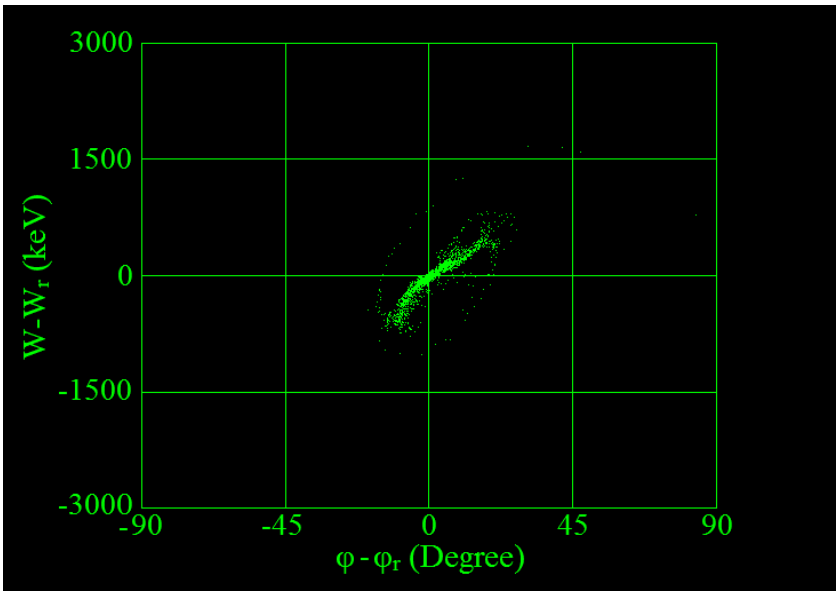

Figure 5: Phase diagram of the main bunch

The data coming from this model could be used for the RF design of the TW buncher and also for the further study of the beam loading of fundamental and higher order modes. Figures 6-9 show the required parameters for each cell for the further design. In the equation below, the bunch form factor (Fig. 9) is defined for N particles:

$$F = \frac{1}{N}\sqrt{\left(\sum_{i=1}^{N} cos(\theta_i)\right)^2 + \left(\sum_{i=1}^{N} sin(\theta_i)\right)^2}$$

Parameter	Value
$Bunch\ length(mm)$	7.23
$Beam\ energy\ sperad(MeV)$	0.317
$Average\ beam\ energy(MeV)$	2.38
Satellite population (%)	2.8

Table 1: The beam properties at the end of the TW buncher

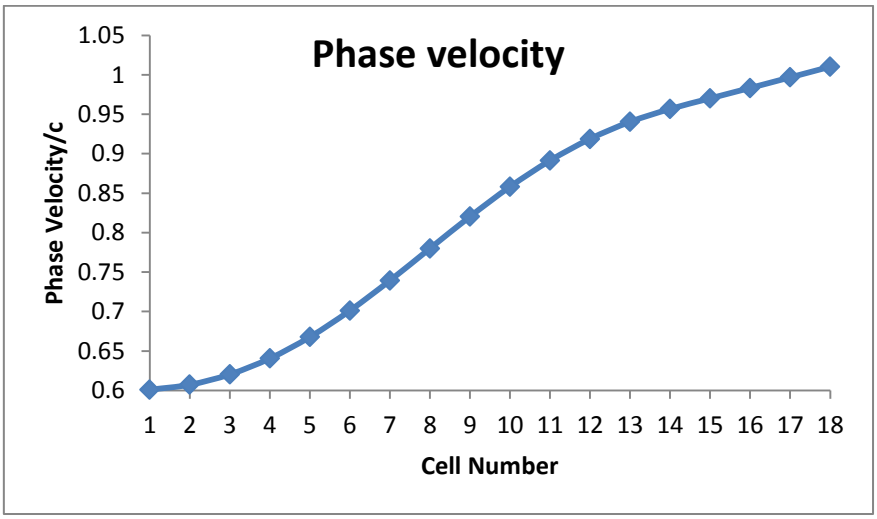

Figure 6: Phase velocity in each cell

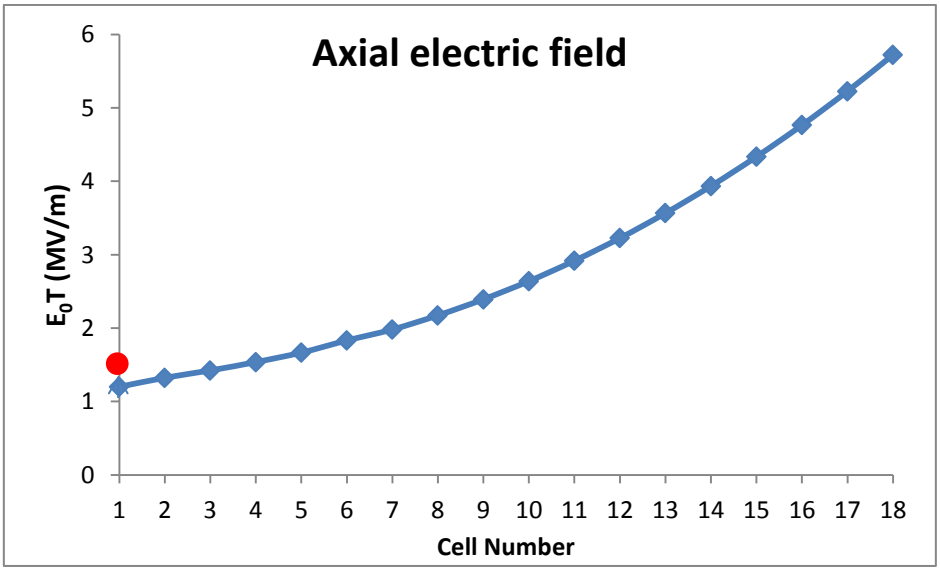

Figure 7: Axial electric field in each cell (for the main harmonic). The red point shows a correction because of the coupler cell

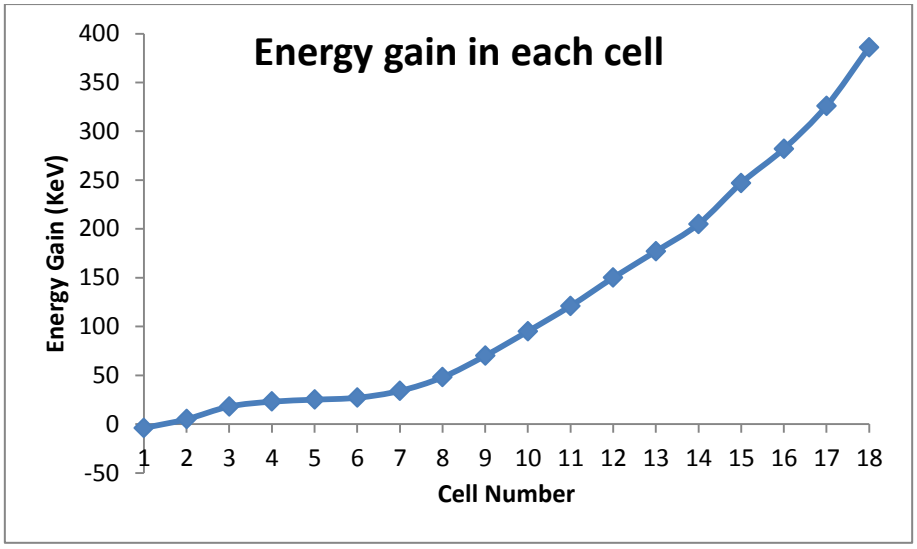

Figure 8: Beam energy gain in each cell

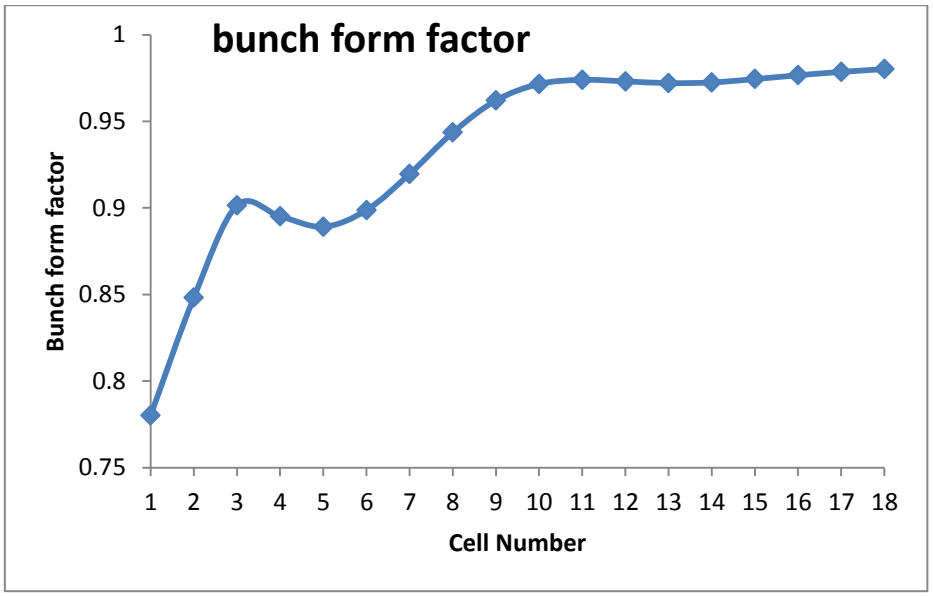

Figure 9: Bunch form factor in each cell

RF design

Normalized electric field

A 20MW klystron feeds the structure and about 19MW RF peak power is available for the TW buncher due to the power loss inside the waveguides and connectors. The beam current is 5A then we can calculate the absorbed power in each cell based on the data shown in the figure 8(Fig. 10) and also the power entering to each cell (Fig.11). To simplify the design, the non-beam-loaded lossless electric field of each cell is used that we call normalized electric field by definition.

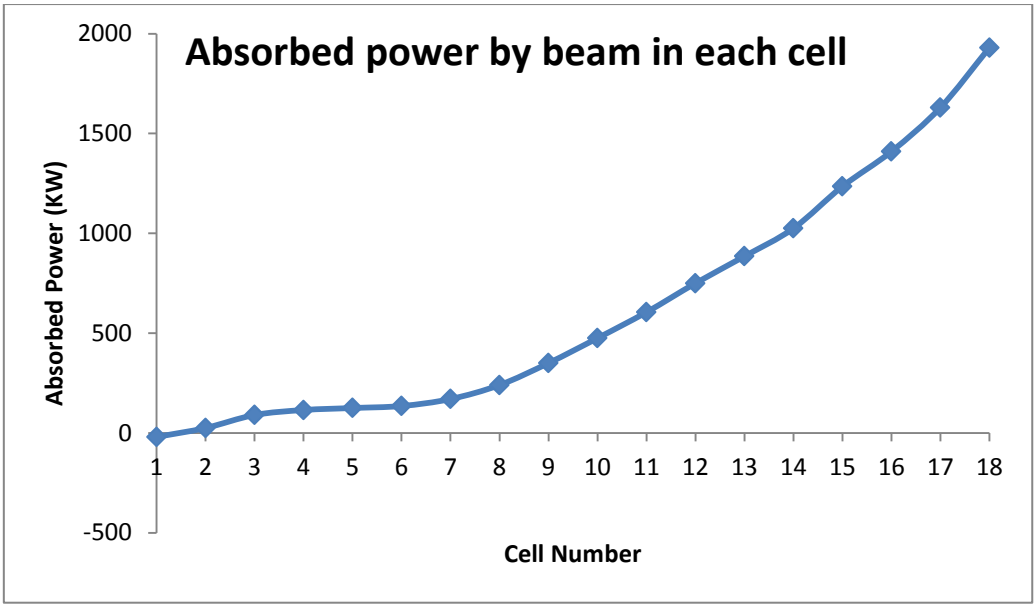

Figure 10: Absorbed power by beam in each cell

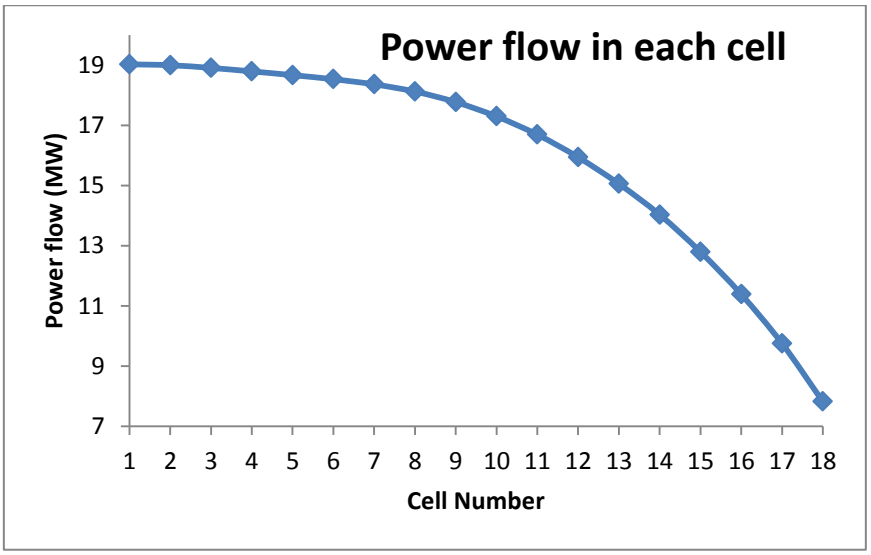

Figure 11: The entering power to each cell

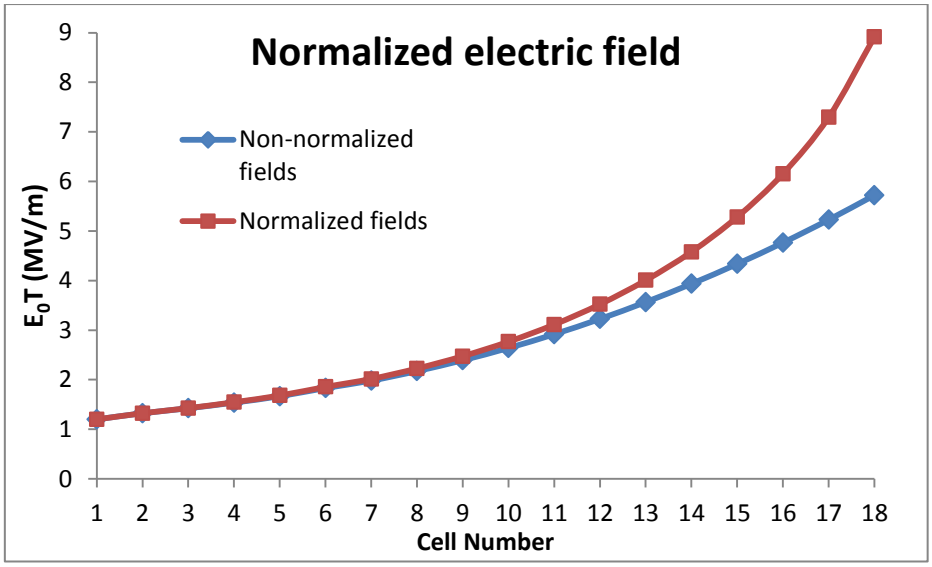

Figure 12: Normalized vs non-normalized axial electric fields

Attenuation effect

Figure 12 shows the normalized field before the surface power loss correction. The equation below shows the power loss on the wall:

$$\begin{cases} \frac{dP}{P} = -2\alpha dz \\ \alpha = \frac{\omega}{2Q_0 v_g} \end{cases}$$

Figure 13 shows the corrected normalized field and you can the difference is so small. The total power loss on the wall is about 0.7 MW (≈ 3.8%) in comparison to the beam absorbed power 11.2MW (≈ 59 %).

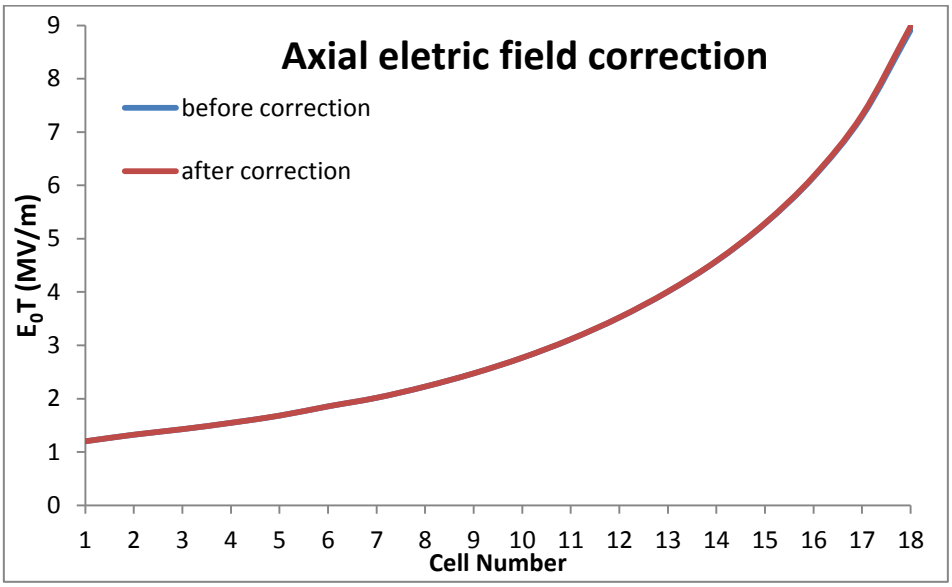

Figure 13: Normalized field correction based on the power loss on the wall

Phase velocity correction based on the fundamental mode reactive beam loading

Another correction for the phase velocity is required based on the reactive beam loading of the fundamental mode. This effect is emerged because the beam is travelling off crest and the high beam current (5A). This effect was studied previously and you can look at it for more details [3]; briefly, the amount of required detuning for a traveling wave structure is equal to a standing wave case done by P. B. Wilson [4] with this assumption that the beam excites mostly the mode that its phase velocity is equal to the beam velocity (Synchronous mode). The equation below shows the corrected phase velocity based on this effect:

$$\begin{cases} \dfrac{\dfrac{1}{v_e}-\dfrac{1}{v_p}}{\dfrac{1}{v_g}-\dfrac{1}{v_e}} = -\dfrac{1}{2\pi}\dfrac{E_{b0}\sin(\varphi_b)}{E_g} \\ E_{b0} = -F\dfrac{\omega_0}{2}\dfrac{r}{Q_0}q \approx -\pi F\dfrac{r}{Q_0}I \end{cases}$$

To do this correction a preliminary design of cells is required. The 5 cells (1, 5, 9, 13, and 17) were designed to find the parameters required for the equation above and the rest cell parameters were found by interpolation. Figure 14 shows the phase velocity correction. It shows that this correction is so small in the first half section that the bunching process is more important.

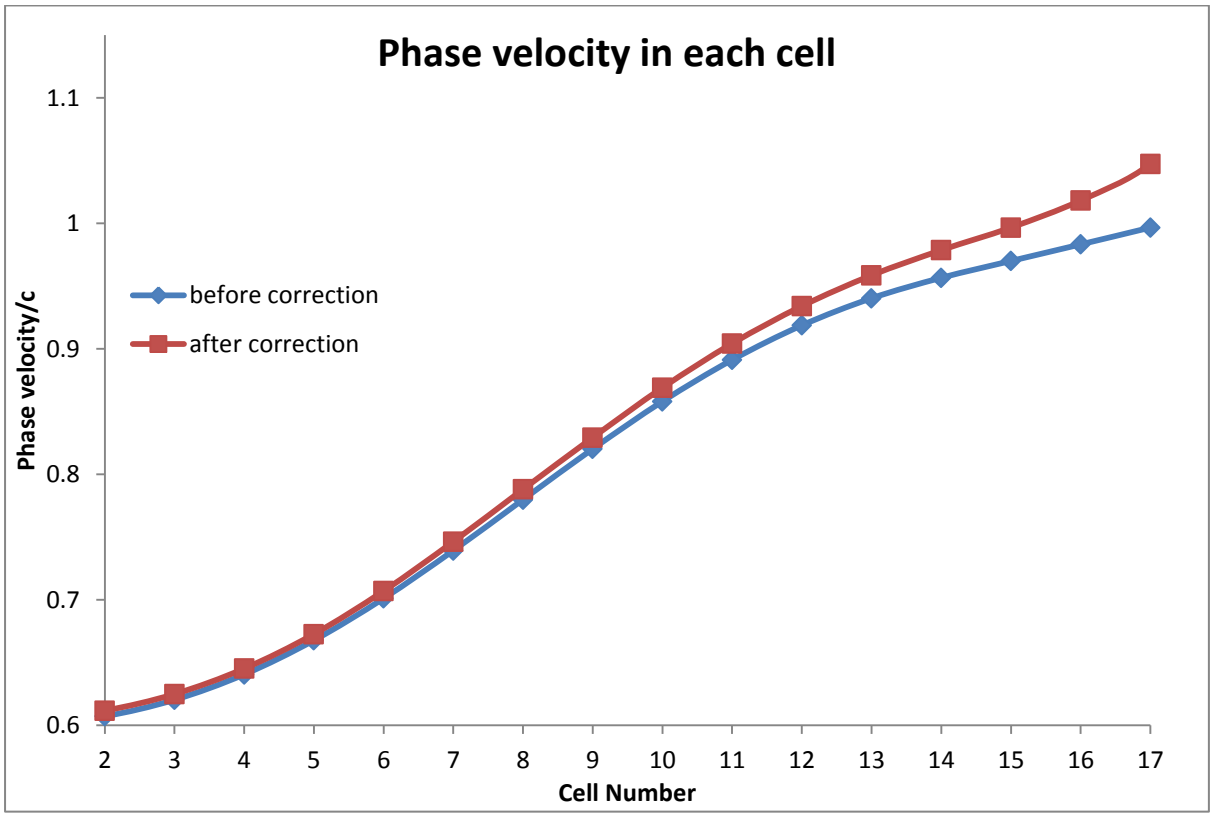

Figure 14: The phase velocity correction based on the reactive beam loading of the fundamental mode

Cells design

As mentioned previously, to finalize the cell design four geometric parameters are needed for each cell: 1-Length (d_i) 2-Inner radius (r_i) 3- Disk aperture radius (a_i) 4- Disk thickness (t=10mm). The cell length is dependent on the phase velocity of the traveling wave inside the cell (v_p), traveling wave frequency (f) that is equal to 999.5MHz and the phase advance between cells (ϕ) that is equal to 2π/3.

$$d = \frac{v_p}{f} \times \frac{\varphi}{2\pi} = \frac{\beta_p c}{f} \times \frac{\varphi}{2\pi}$$

The magnitude of the axial electric field is mostly dependent on the disk aperture radius that was modified to reach our desired electric field. The inner cell radius is finally chosen to keep the phase advance equal to 2π/3 for the traveling wave frequency equal to 999.5MHz. Figure 15 shows one cell layout.

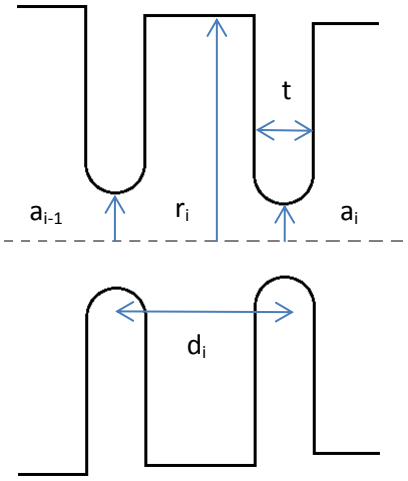

Figure 15: The cell layout.

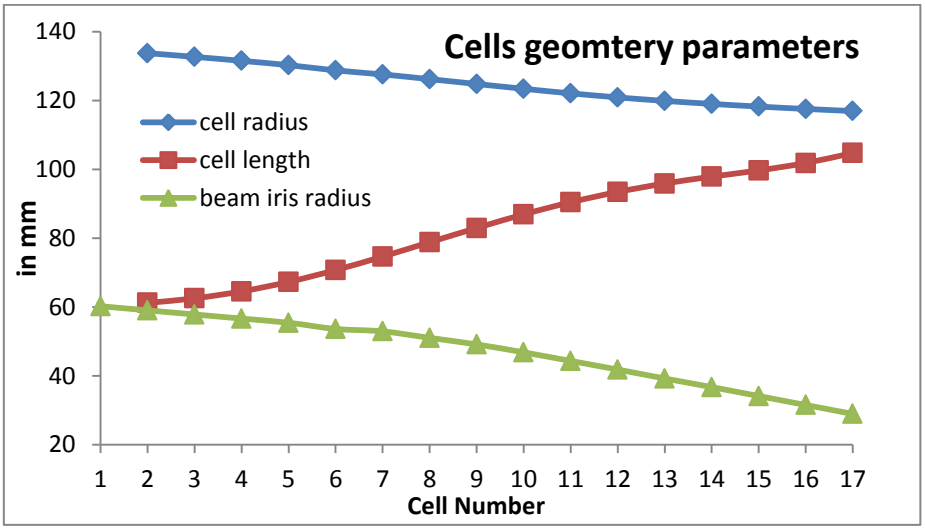

Figure 16: Cells geometry parameters for all cells except the coupler cells

Cell Number	Disk Aperture Radius(mm)	Cell Radius(mm)	Cell Length(mm)
1	60.2		
2	59	133.72	61.172
3	57.8	132.65	62.487
4	56.6	131.49	64.516
5	55.4	130.25	67.262
6	53.6	128.72	70.7
7	52.9	127.55	74.628
8	51	126.18	78.797
9	49.1	124.77	82.921
10	46.8	123.37	86.895
11	44.3	122.05	90.414
12	41.8	120.88	93.398
13	39.2	119.86	95.849
14	36.7	118.99	97.852
15	34.1	118.21	99.655
16	31.5	117.52	101.812
17	28.9	116.91	104.719

Table 2: Cells geometry parameters for all cells except the coupler cells

Now by knowing the normalized field and the phase velocity for each cell that was shown in the previous section we can design the cells. Figure 16 and Table 2 shows the geometrical parameters for all cells except the coupler cells that we talk about them in next sections.

Figure 17 shows the group velocity for each cell. Until the middle of the TW buncher the group velocity is mostly constant and then it decrease mostly linearly to reach about 0.01c. Less group velocity means more sensitivity and more beam loading and HOMs effect but is unavoidable because we should decrease the group velocity to reach the desired shunt impedance for each cell.

Figure 18 shows the shunt impedance over Q for each cell. It was increased during the structure because we need more axial electric fields with less flowing power.

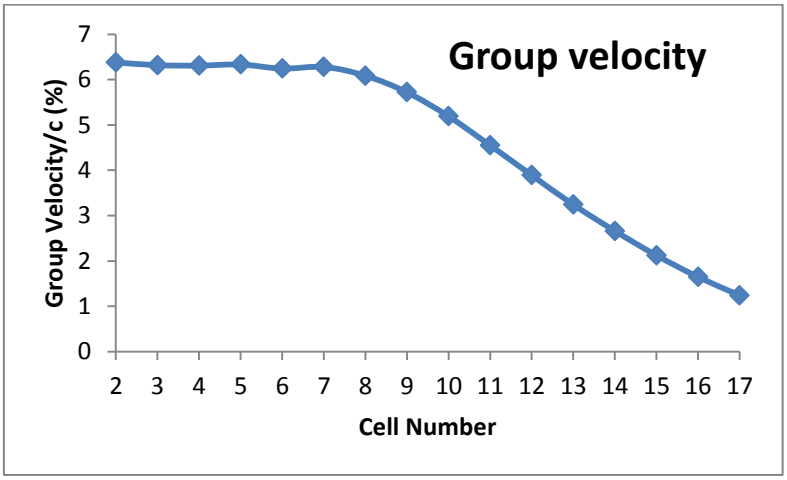

Figure 17: Group velocity for all cells except the coupler cells.

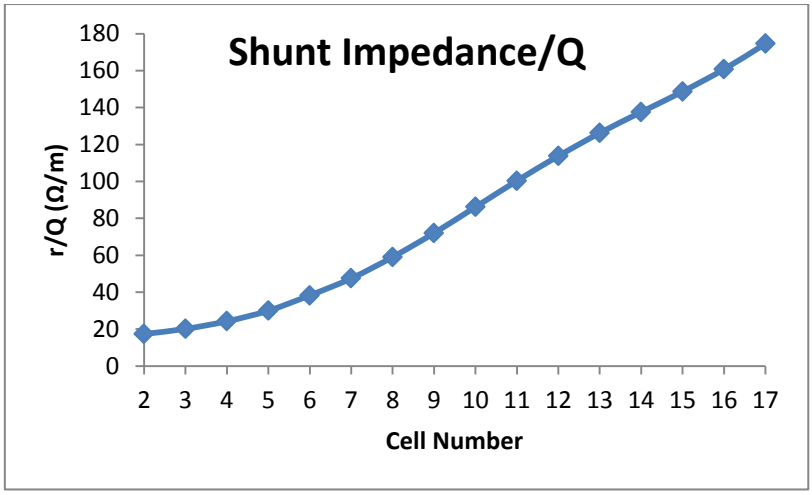

Figure 18: Shunt impedance over Q for all cells except the coupler cells.

Input coupler (double feedings)

To connect the WR975 rectangular waveguide to the TW buncher we should design the power couplers. A tapered waveguide connected the WR975 waveguide to the coupler cell and a slot is opened to let the RF wave enters the coupler cell (Fig. 19). Now, a proper slot size and the coupler cell radius should be found to match these two structures and to avoid any internal reflection. Figure 19 shows a setup that we used to match them. Intermediate cells are similar to the cell 2 except that the disk apertures radius are equal and the inner radius is a bit changed for the proper phase advance. Three similar setups are used with different number for the intermediate cells (three, four and five). For each slot size and the coupler cell radius, these three setups are simulated to find the reflection (S11) of each dimension. The reason to use three setups is to avoid the low S11 due to partial cancelation of two reflecting waves from the input and output couplers. Then for each dimension, the maximum S11 between these three setups are taken. The best dimension is the one with the lowest S11.

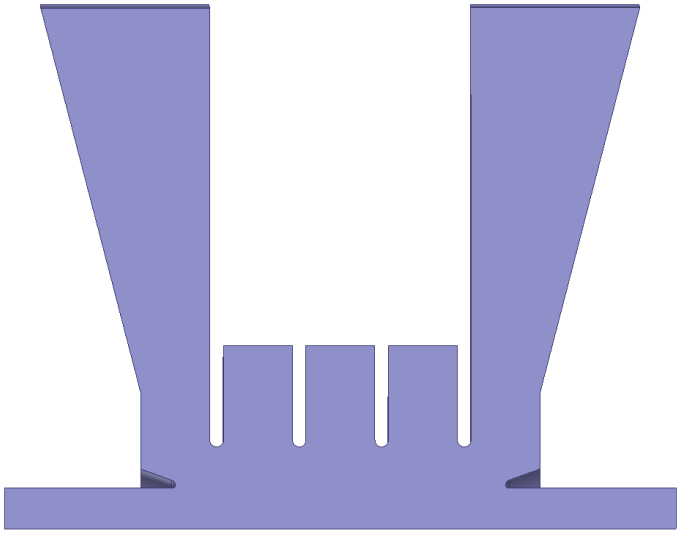

Figure 19: A setup with two input couplers and the intermediate cells

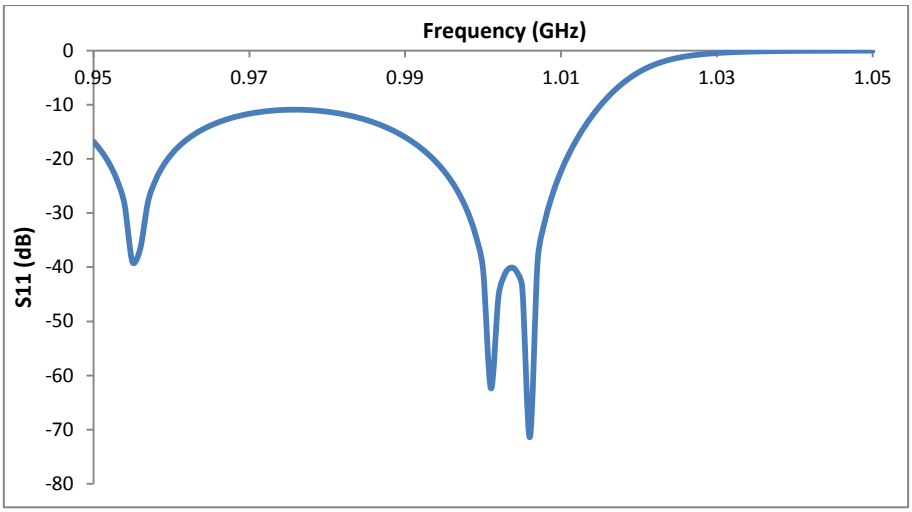

Figure 20: S11 diagram for the matched setup

Figure 19-21 show the result for the matched structure. In this design, a bump is placed around the entering beam tube (Fig. 19). This helps to decrease the field seen by the beam when enters the structure or in other words, to avoid the entrance standing pattern field. Figure 22 shows the field seen by a bunch when it enters the structure.

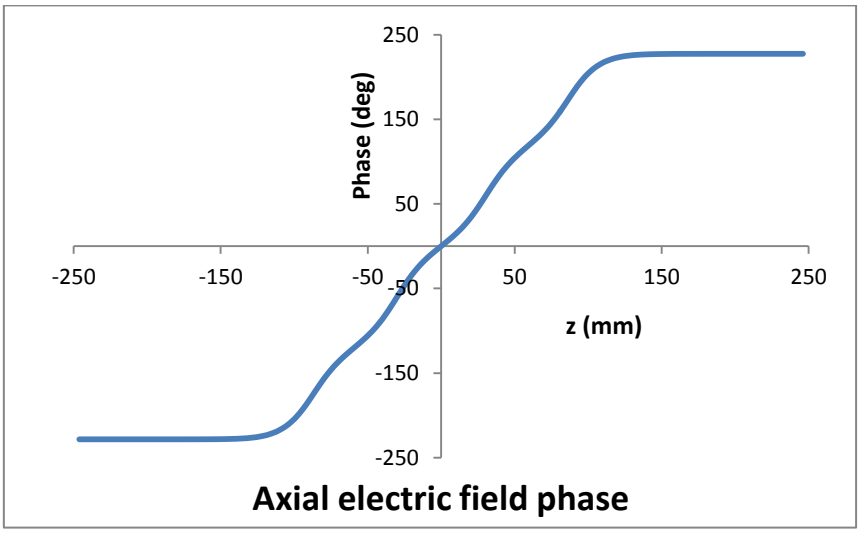

Figure 21: Axial electric field phase for the matched setup

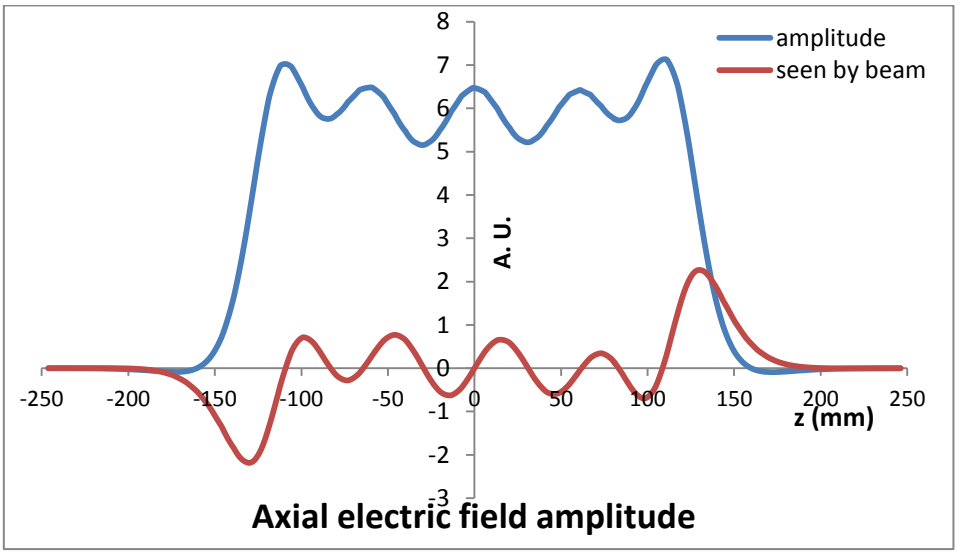

Figure 22: Axial electric field amplitude for the matched setup. Red line shows the electric field seen by the entering bunch.

Output coupler (double feedings)

The process to design the output coupler cell is similar to the input coupler design except we don't use the bump around the beam tube because the beam energy is high enough and the exit standing pattern fields seen by a bunch doesn't disturb it. The intermediate cells are similar to the cell 17 except that the disk apertures radius are equal and the inner radius is a bit changed for the proper phase advance.

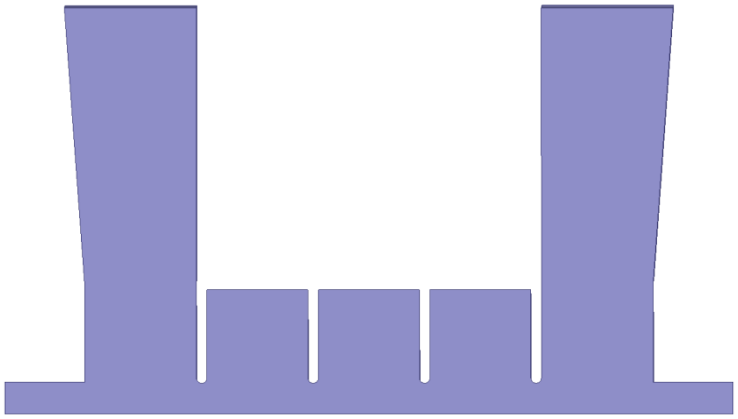

Figure 23: A setup with two output couplers and the intermediate cells

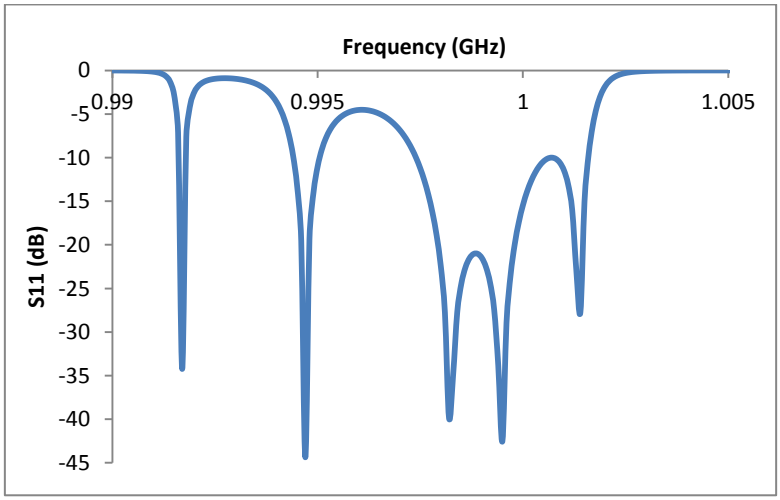

Figure 24: S11 diagram for the matched setup

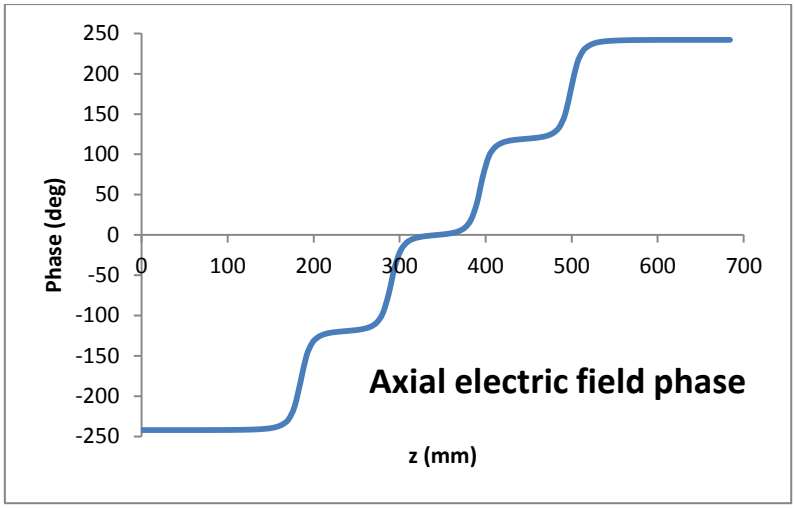

Figure 25: Axial electric field phase for the matched setup

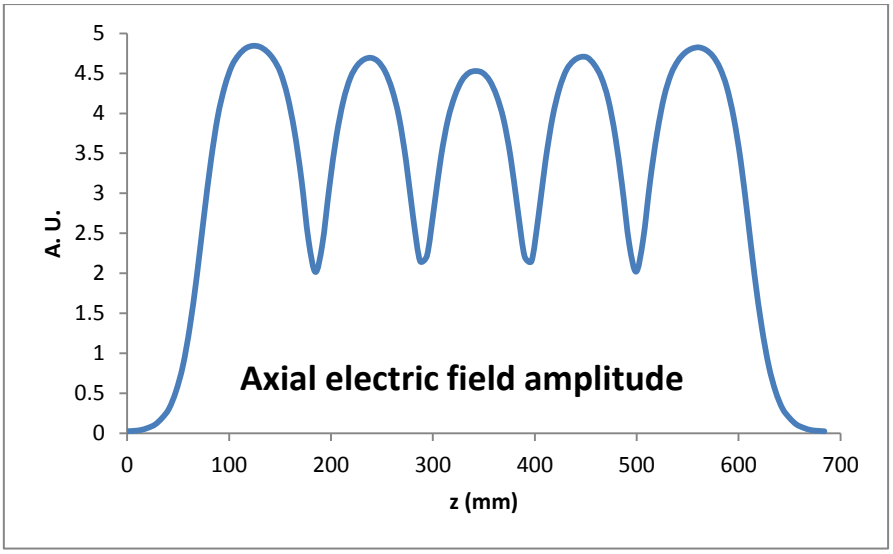

Figure 26: Axial electric field amplitude for the matched setup

Full structure result

By using the input and the output coupler cells, the full structure can be simulated (Fig. 27). Figures 28-30 show the reflection and the axial electric field. Figures 27 and 28 also show a little local reflection inside the structure. Because of tapering structure, some local reflection is unavoidable but the result could be better by retuning a few intermediate cells (like cells 12, 14, 15, 17) and rematching the couplers. Another option is to remove the one or two last cells. It decreases the local reflection with a minor effect on the beam properties.

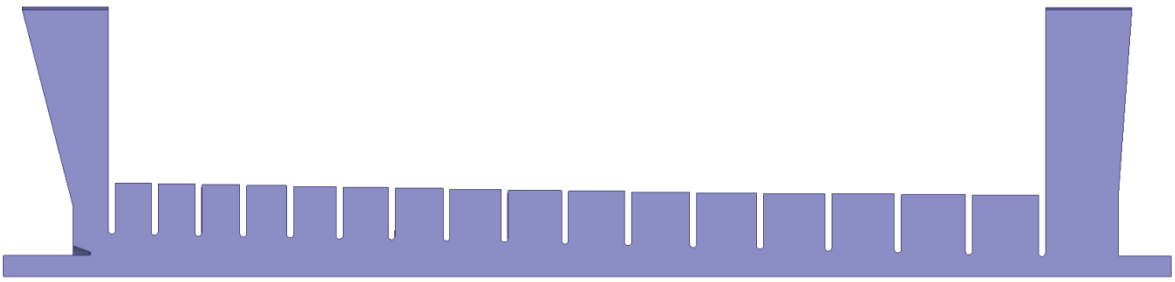

Figure 27: The full structure setup

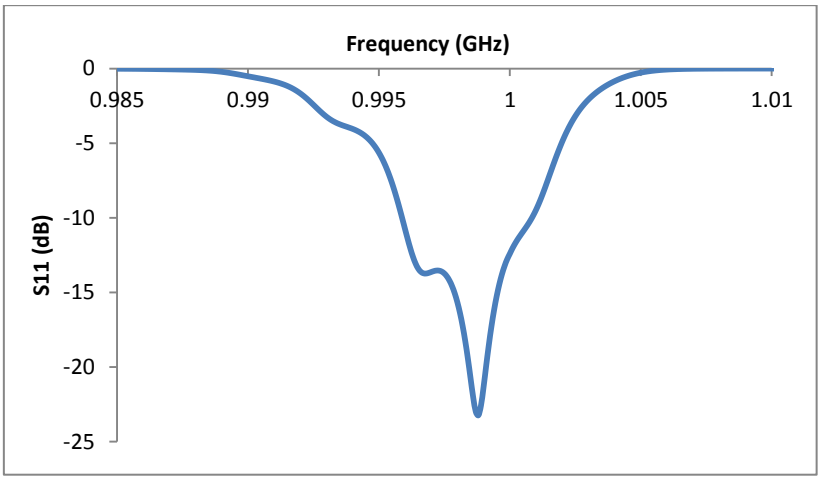

Figure 28: S11 diagram for the full structure

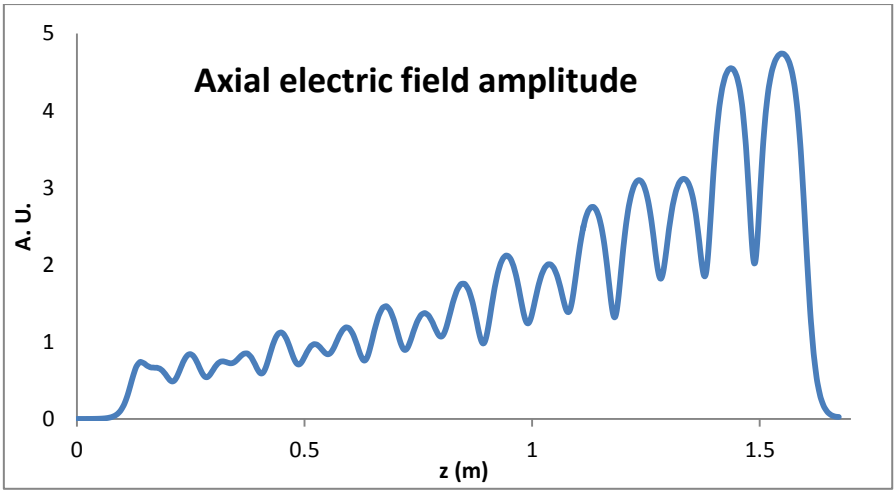

Figure 29: Axial electric field amplitude for the full structure

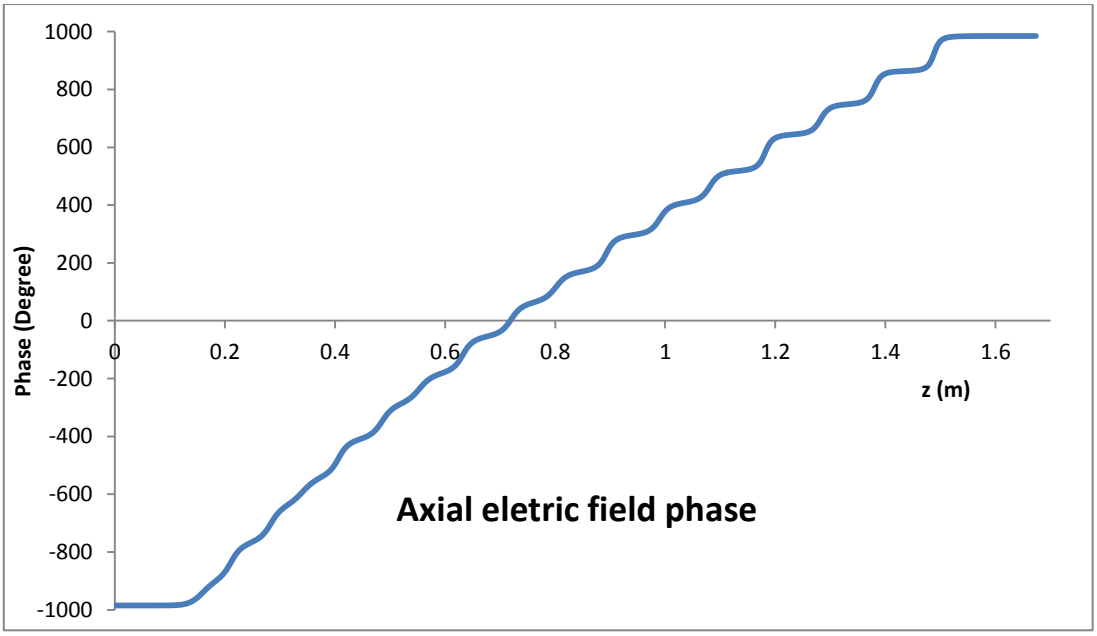

Figure 30: Axial electric field phase for the full structure

HOMs study

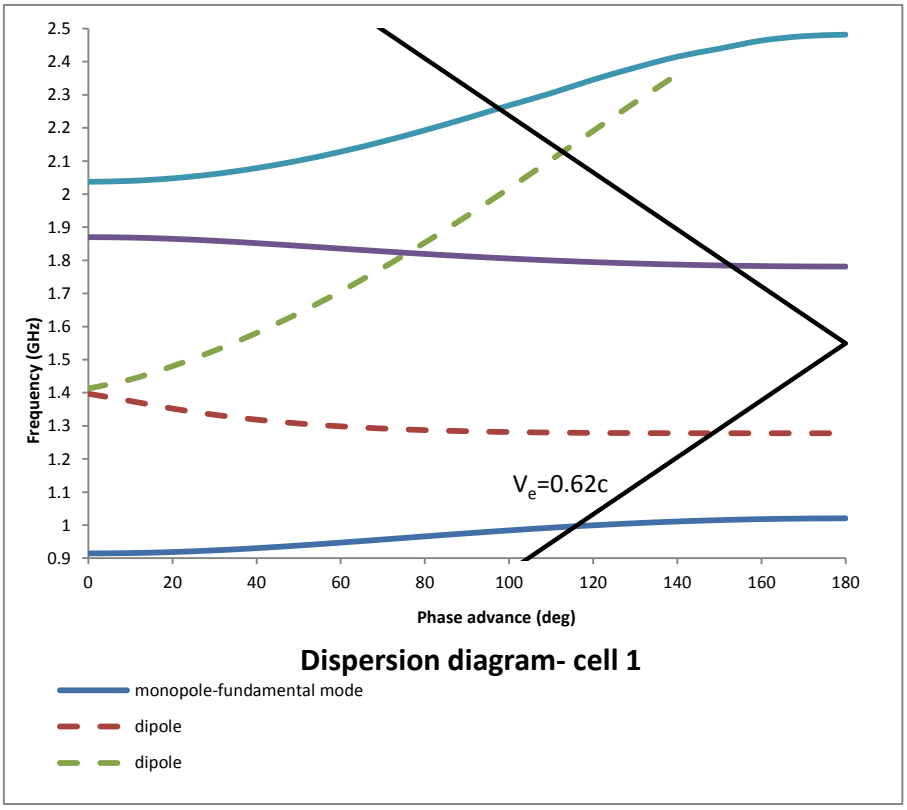

Figure 31: The dispersion diagram for the cell no.1

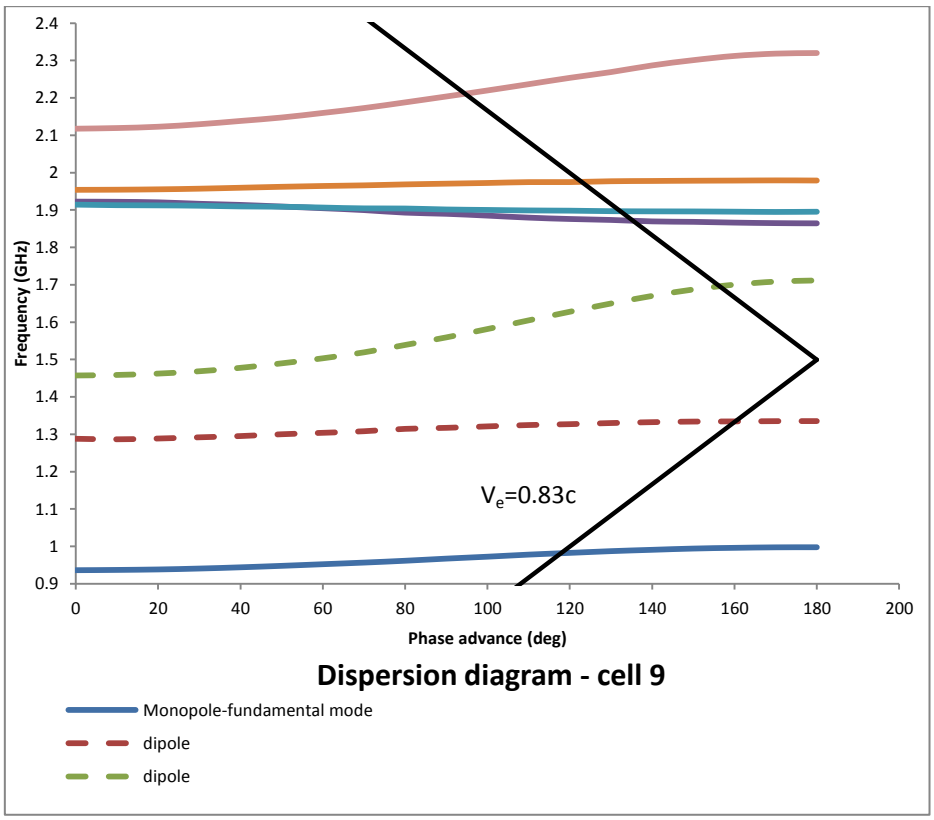

Figure 32: The dispersion diagram for the cell no.9

To finalize the full structure RF design it should be shown if the HOMs dampers are required or not. Figure 31-33 shows the dispersion diagram for three different cells in the structure. The beam excited mostly the modes that their phase velocity is equal to the beam velocity (Synchronous modes). These modes could be dangerous if their frequency is close to 0.5 GHZ (beam frequency) or an integer multiplication of it (bunch harmonics). The structure is heavily tapered then there is natural detuning between modes excited in each cell. At first glance, the diagrams shows the HOMs dampers are not required but it needs more study to be completely sure.

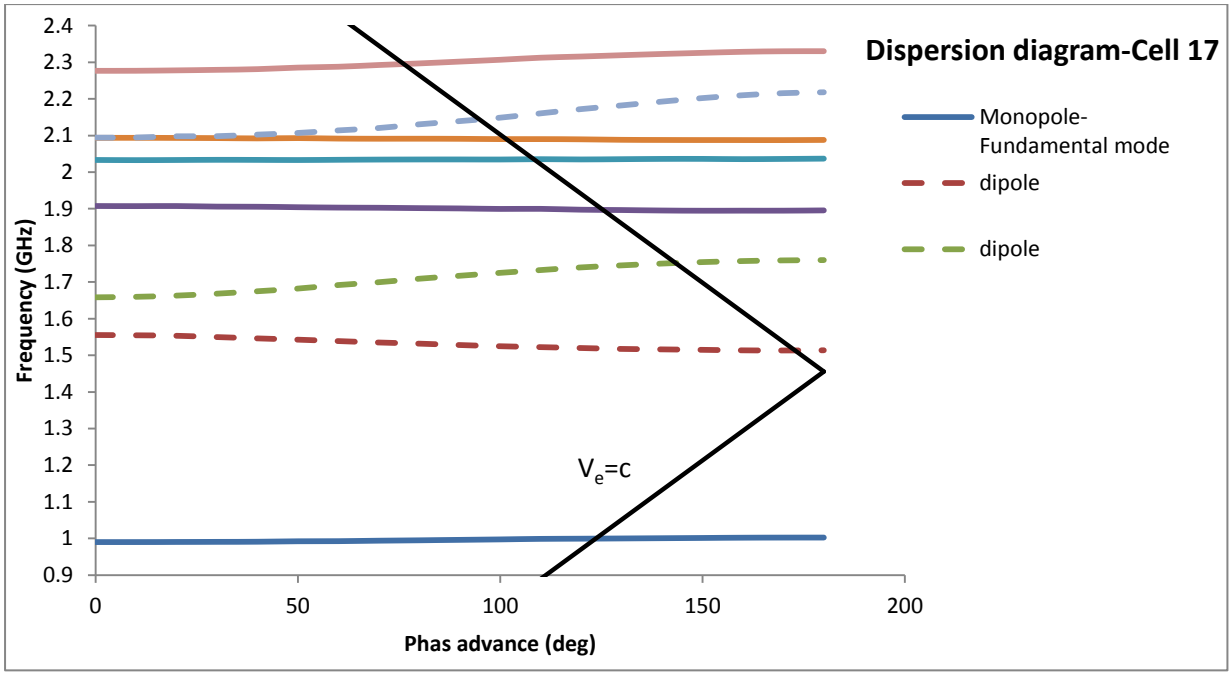

Figure 33: The dispersion diagram for the cell no.17

Conclusion and the future works

The preliminary RF design of the full structure is done. Some retuning of a few cells and rematching of the couplers are required to reach less internal reflection. It also seems that the HOMs dampers are not required due to the natural detuning between cells but the further study for the HOMs effect is necessary to be completely sure. A sensitivity analysis will be performed to determine mechanical tolerances. Full 3D models in HFSS have been used for the design and are available for a future mechanical design.

References

1- Beam Dynamics Studies of the CLIC Drive Beam Injector complex, S. Sanaye Hajari et al., LINAC 14, Geneva, Switzerland 2014
2- A Multi-TeV Linear Collider Based on CLIC Technology: CLIC Conceptual Design Report, CERN-2012-007, M. Aicheler et al.
3- General Beam Loading Compensation in a Traveling Wave Structure, H. Shaker et al., IPAC13, Shanghai, China 2013
4- High Energy Electron Linacs: Applications to Storage Ring RF Systems and Linear Colliders, P. B. Wilson, SLAC PUB-2884, Feb 1982